Supplementary Fig. 1. The effect of triton X-100 concentrations on MERS-CoV 3CLpro. Each bar represents the proteolytic activity of MERS-CoV 3CLpro depending on the concentrations of triton X-100. Each bar is expressed as the mean ± standard error of the mean (n = 3). RFU = Relative Fluorescence Units

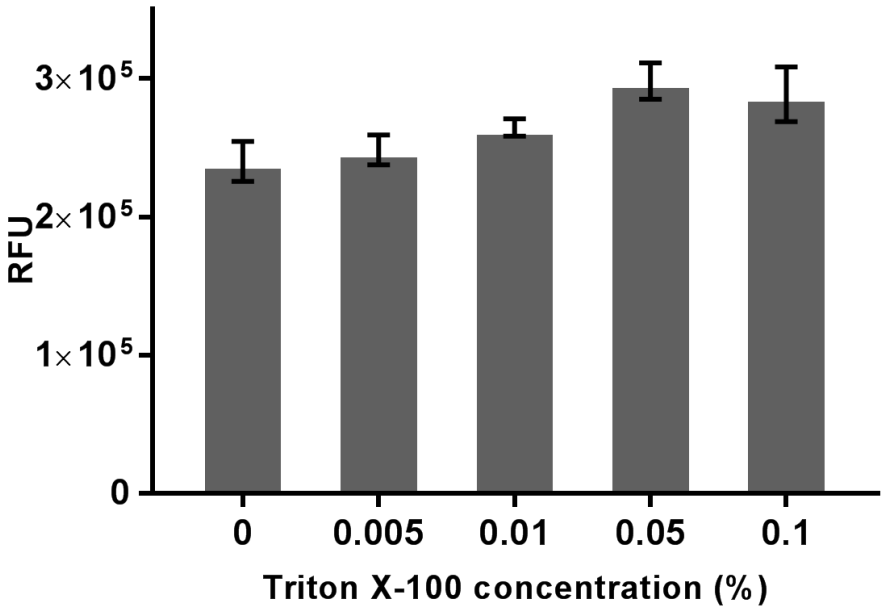

Supplementary Fig. 2. Chemical structures of the inhibitory compounds and their homologs. Homologs of helichrysetin, herbacetin, isobavachalcone and quercetin 3-β-D-glucoside are cardamonin, kaempferol, 2,2′,4′-trihydroxychalcone and quercitrin, respectively.

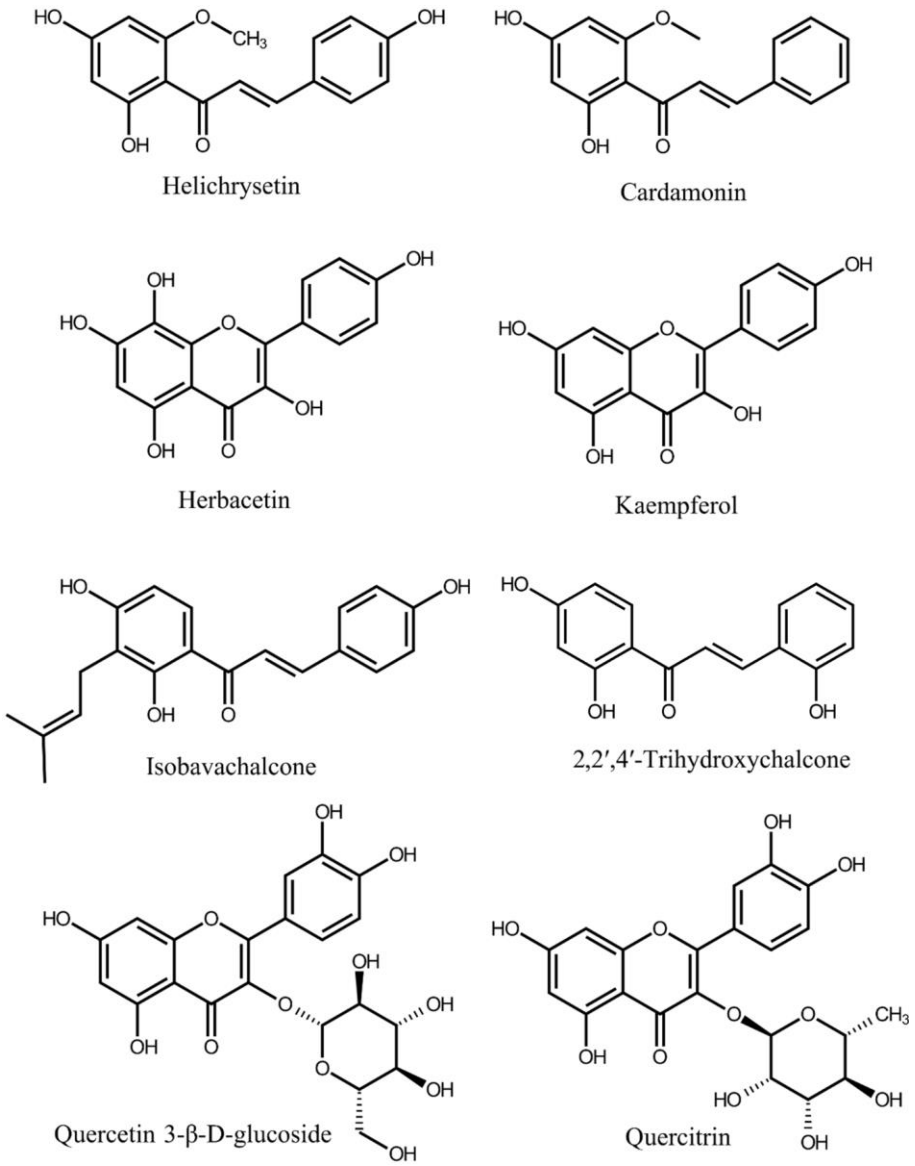

Supplementary Fig. 3. Predicted complexes of flavonoids in the catalytic site of MERS-CoV 3CLpro. Docking poses of (A) helichrysetin and cardamonin (B) herbacetin and kaempferol (C) isobavachalcone and 2,2′,4′-trihydroxychalcone (D) quercetin 3-β-D-glucoside and quercitrin were depicted on the electrostatic surface potential of MERS-CoV 3CLpro (red, negative; blue, positive; white, uncharged). Flavonoids are predicted to occupy the active site of MERS-CoV 3CLpro where the catalytic dyad, Cys148 and His41 (labeled with red color), is located. 2D schematic representations of the interactions of eight flavonoids are also drawn. Figures were created with Maestro v11.5.011. S1 represents the S1 site of MERS-CoV 3CLpro where Cys148 locates and S2 for the hydrophobic S2 site. The pink arrows represent hydrogen bond interaction and the green dotted lines for π-π stacking interaction.

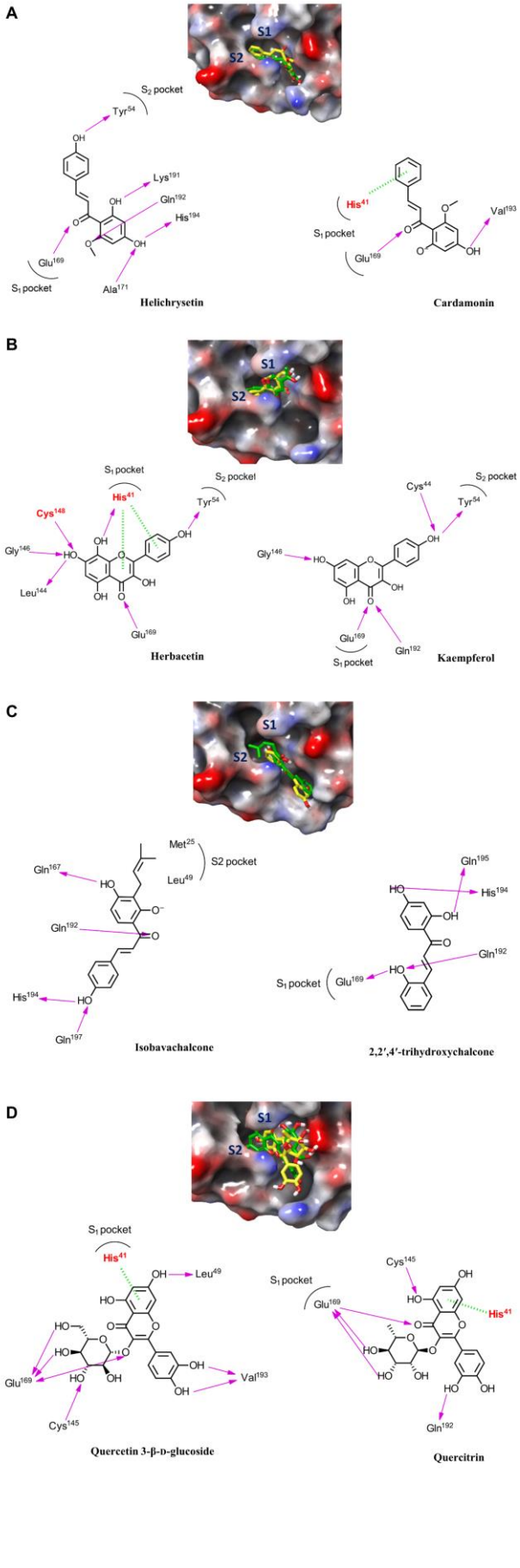
A
S1
S2
S2 pocket
Tyr54
Lys191
Gln192
His194
Glu169
S1 pocket
Ala171
Helichrysetin
His41
S1 pocket
Glu169
Val193
Cardamonin
B
S1
S2
S1 pocket
His41
S2 pocket
Tyr54
Cys148
Gly146
Leu144
Glu169
Herbacetin
Cys44
S2 pocket
Tyr54
Gly146
Glu169
S1 pocket
Gln192
Kaempferol
C
S1
S2
Met25
S2 pocket
Leu49
Gln167
Gln192
His194
Gln197
Isobavachalcone
Gln195
His194
Gln192
S1 pocket
Glu169
2,2′,4′-trihydroxychalcone
D
S1
S2
S1 pocket
His41
Leu49
Glu169
Val193
Cys145
Quercetin 3-β-D-glucoside
S1 pocket
Cys145
Glu169
His41
Gln192
Quercitrin

Supplementary Fig. 4. Superimposed structures of the protease domains of three viral proteases. The ribbon diagrams are depicted using different colors to represent three viral proteases, MERS-CoV 3CLpro (PDB: 4WMD) (light green), dengue virus NS2B/NS3 protease (PDB: 2FOM) (pink) and norovirus 3C-like protease (PDB: 1WQS) (sky blue). The root-mean-square deviations (RMSDs) of the catalytic domain of MERS-CoV 3CLpro with those of dengue virus NS2B/NS3 protease (53 Cα atoms) and norovirus 3C-like protease (45 Cα atoms) are 1.057 and 0.944, respectively. Most of the catalytic residues of MERS-CoV 3CLpro (C148A, H41), dengue virus (S135, H51, D75) and norovirus (C139, H30) are well aligned. The enlarged view of the right figure of the active sites was obtained after 45˚ rotation along the X-axis. The N- and C-terminal of the catalytic domain of MERS-CoV 3CLpro were labeled on the first (S10) and the last (L198).